RSC Advances

PAPER

View Article Online
View Journal | View Issue

Cite this: *RSC Adv.*, 2015, **5**, 44274

Tuning the thermotropic properties of liquid crystalline *p*-substituted aroylhydrazones†

Hemant Kumar Singh,[a] Sachin Kumar Singh,[a] Rajib Nandi,[b] Madan Kumar Singh,[a] Vijay Kumar,[a] Ranjan K. Singh,[b] D. S. Shankar Rao,[c] S. Krishna Prasad[c] and Bachcha Singh*[a]

Received 13th April 2015
Accepted 8th May 2015

DOI: 10.1039/c5ra06620d

www.rsc.org/advances

The synthesis and mesomorphic properties of forty substituted aroylhydrazones with peripheral mono-, di- and tri- alkoxy chains derived from a *p*-amino aroylhydrazone core are described. The compounds with two side chains exhibited a smectic A phase, while the compounds with six soft alkoxy side chains at symmetrical positions formed a rectangular columnar mesophase. The structures of these mesophases were confirmed by differential scanning calorimetry (DSC) analysis, polarized optical microscopy (POM) and powder X-ray diffraction (XRD) studies. Raman studies with the help of density functional theory on some of the mesogenic members have been performed to understand the changes in the intermolecular interactions during phase transitions. A structure–property relationship has been deduced, and mesogenic properties are found to be dependent on the chain length, density and position of the alkoxy chains around the molecular core.

1. Introduction

Aroylhydrazones, hydrazine derivatives and their metal complexes are some of the most versatile compounds that exhibit a broad spectrum of biological, bactericidal and fungicidal activities and are of great interest due to their analytical, industrial and pharmacological importance.[1–7] These compounds can also manifest a wide spectrum of functional properties such as redox activities, magnetism, luminescence, supramolecular order, sensing probes, *etc.*[8–11] Several synthetic methodologies have been developed in the past to functionalize the aroylhydrazone core at different ring positions.[12–17] The aroylhydrazone core (–C_6H_5–C(=O)–NH–N=CH–C_6H_5–) has, benzoyl (–C_6H_5C=O–) and benzylidene (=CH–C_6H_5–) terminals for easy incorporation of various suitable substituent and derivatives. By proper design of the aroylhydrazone derivatives, it is possible to obtain different types of liquid crystals (LCs) and tune their mesomorphic potential, although examples of mesogenic aroylhydrazones are very few. It was firstly explored by McCabe *et al.* by design and synthesis of a series of nickel(II) and copper(II) complexes of aroylhydrazone derivatives (Fig. 1A). The mesomorphic nature of these complexes was found to be strongly dependent on the nature of the substituent at the azomethine moiety.[18,19] Lai *et al.* synthesized a series of polycatenar aroylhydrazinato-nickel(II) metallo-mesogens showing columnar mesophases (Fig. 1B). These derivatives showed interesting mesophase crossover phenomenon from rectangular to hexagonal columnar phase with increasing alkoxy chain length.[20] Tschierske and Yelamaggad have reported interesting room temperature mesophase of aroylhydrazones (Fig. 1C). They combined 3,4,5- and 2,3,4-trialkoxy substitution patterns on benzoyl- and benzylidene units respectively, to obtain low melting columnar LC materials. The mesophase of these derivatives were found due to adaptation of unusual supramolecular helical organization of molecules by intermolecular hydrogen bonding.[21] Recently, our group has reported calamitic mono- and disubstituted aroylhydrazone derivatives showing variety of mesophases depends on their terminal substitution patterns (Fig. 1D).[22–25]

In this work, we synthesized rigid, extended, mono- to tricatenar alkoxy systems derived from aroylhydrazones. The aroylhydrazone unit was extended in the *p*-benzoyl-position using imine linking group. The mesophase behavior of these compounds was investigated as a function of chain length, density and position of alkoxy tails. Mesophase crossover from typical smectic A (SmA) to rectangular columnar (Col_r) mesophase was found in these derivatives and investigated in detail by polarising optical microscopy (POM), differential scanning calorimetry (DSC) and powder X-ray diffraction (XRD) studies. Also the nature of inter-amide hydrogen bonding (–C=O···H–N–) during phase transitions (crystal → mesophase) was investigated by Raman spectroscopic studies.

---

[a] *Department of Chemistry (Centre of Advance Study), Faculty of Science, Banaras Hindu University, Varanasi-221005, India. E-mail: bsinghbhu@rediffmail.com*

[b] *Department of Physics (Centre of Advance Study), Faculty of Science, Banaras Hindu University, Varanasi-221005, India*

[c] *Centre for Nano and Soft Matter Sciences, Jalahalli, Bangalore-560013, India*

† Electronic supplementary information (ESI) available. See DOI: 10.1039/c5ra06620d

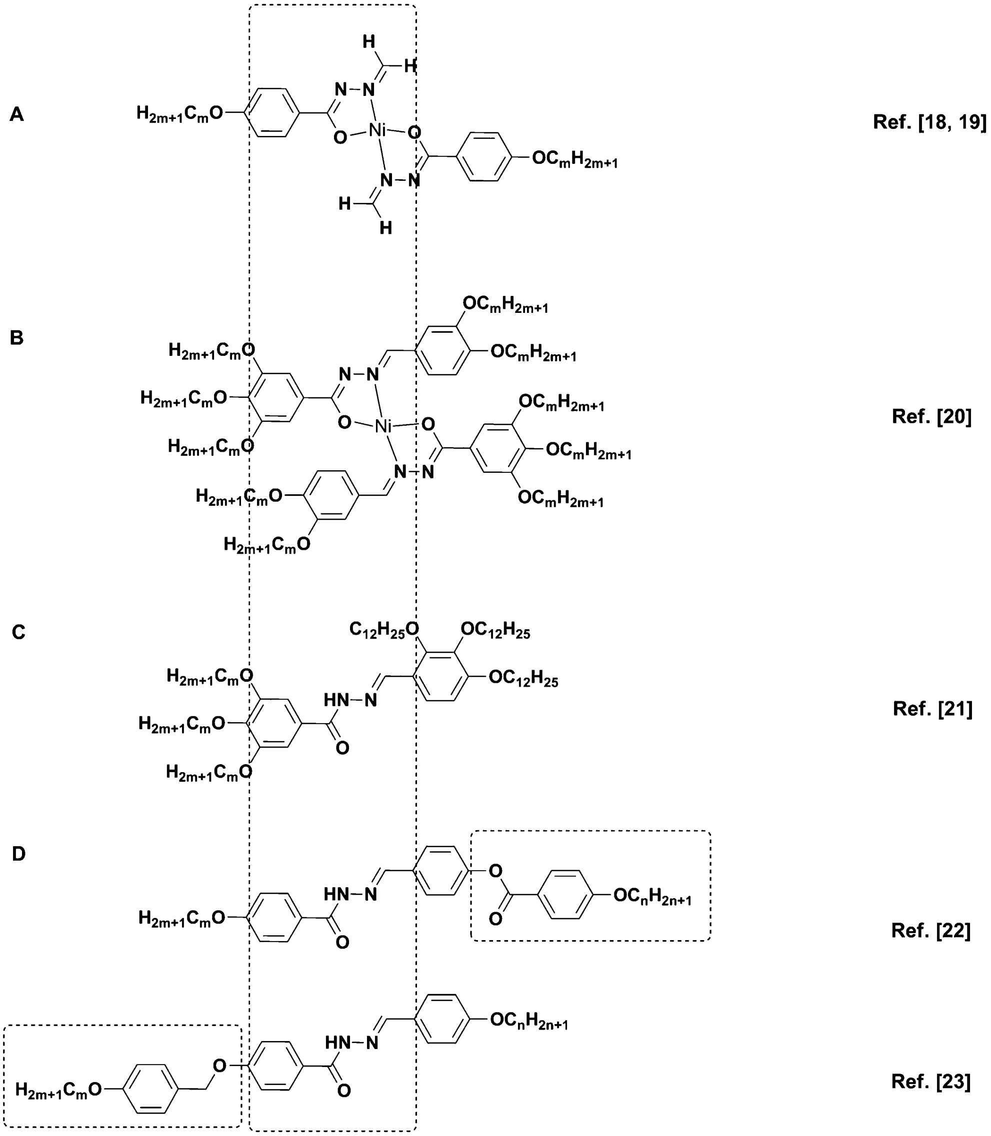

Fig. 1 (A) Mesogenic mono-alkoxy aroylhydrazone-nickel(II) complex reported by McCabe *et al.*[18,19] (B) Polycatenar aroylhydrazone-nickel(II) complexes reported by Lai *et al.*[20] (C) Structure of non-symmetrical polycatenar aroylhydrazones reported by Yelamaggad *et al.*[21] (D) Substituted aroylhydrazones at benzylidene-[22] and benzoyl- position[23] reported by Singh *et al.*

2. Results and discussion

2.1 Synthesis

The synthetic route for preparation of aroylhydrazone based ligands is outlined in Scheme 1. Alkylation of 4-hydroxybenzaldehyde with 1-bromoalkane in 2-butanone using potassium carbonate leads to formation of 4-alkoxybenzaldehyde.

Reaction of ethyl-4-aminobenzoate with hydrazine hydrate in re-fluxing absolute ethanol gave 4-aminobenzohydrazide as white solid. The Schiff bases were obtained by the condensation reaction of 4-aminobenzohydrazide with appropriate aldehydes in refluxing ethanol. All the ligands were characterized by elemental analyses and standard spectroscopic techniques. The experimental procedures, synthesis of the intermediates and analytical data are described in the ESI.†

2.2 Mesomorphic behaviour of novel substituted aroylhydrazone compounds

The thermotropic behaviour of the title aroylhydrazones were studied by combining thermo gravimetric analyses (TGA), DSC, POM and XRD studies (in selected cases). Transition temperatures and their associated enthalpy, entropy changes are gathered in Tables 1–3. The mesomorphic properties of these compounds are described accordingly two, four and six terminal chains ($n = 5$–16) in the following sections.

2.2.1 Compounds with two terminal chains. TGA measurements performed on these compounds proved good thermal stability up to 250 °C. DSC analysis showed that these compounds exhibit several reversible transitions on the second heating and cooling curve, indicating polymorphic nature of compound (Fig. 2a and b). Such polymorphism has often been

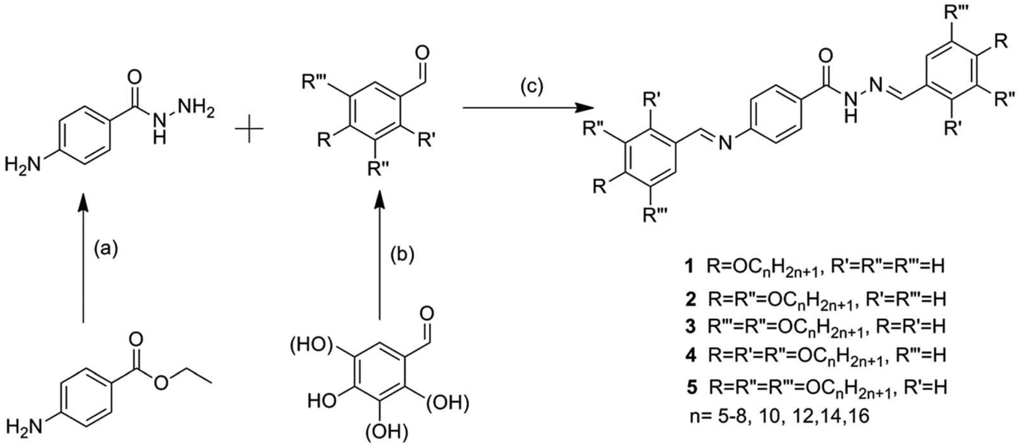

Scheme 1 Reactions and reagents: (a) NH_2NH_2 (1.5 equiv.), refluxing in absolute EtOH, 12 h, 85–90%. (b) RBr (*n* equiv.), K_2CO_3 ($4 \times n$ equiv.), KI (catalyst), refluxing in 2-butanone, 24–72 h, 70–85%. (c) Acetic acid (cat.), refluxing in EtOH, 12 h, 74–87%.

observed in Schiff base containing compounds.[26] NMR experiments also performed after the DSC measurements and revealed that the compounds did not degrade after several temperature cycles up to 250 °C.

In the series of mesogens, **1** ($n = 5$–8, 10, 12, 14, 16) with the moderate alkyl chain length ($n = 12$) at benzylidene moiety shows five endo- and three exothermic peaks in DSC thermogram (Fig. 2a). POM observations reveal that upon heating from crystal state to 171.6 °C, focal conic texture corresponding to SmA mesophase emerges, which further transforms to isotropic liquid at 221.8 °C. In cooling cycle, POM reveals the same textural observations, which emerges from 219.4 °C and solidifies at 162.2 °C. Reheating regenerates the focal conic SmA mesophase with similar pattern; that is, the mesomorphism is enantiotropic (Fig. 3).

The smectic A mesophase behaviour was obtained for the series of compounds **1** with lower and higher alkoxy chain length homologous derivatives ($n = 5$–8, 10, 14, 16) with continuous lowering in melting and clearing temperatures without considerable changes in mesophase temperature range. The mesophase temperature of the compounds ranged 204.8–231.5 °C and 230.5–200.3 °C in heating and cooling cycles, respectively. Table 1 summarizes the thermodynamic parameters associated with the mesomorphic transitions of all the alkoxy benzylidene derivatives.

Table 1 Thermal transitions and corresponding thermodynamic parameters[a]

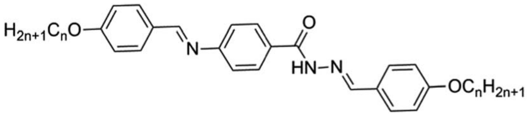

Compound	Heating T, °C [ΔH, kJ mol^{-1}; ΔS, J (mol^{-1} K^{-1})]	Cooling T, °C [ΔH, kJ mol^{-1}; ΔS, J (mol^{-1} K^{-1})]
1 ($n = 5$)	Cr 96.5 (6.8; 18.4) Cr′ 211.1 (45.5; 94.0) SmA 231.6 (5.5; 10.9) i	i 230.5 (−5.2; −10.3) SmA 196.6 (−23.9; −50.9) Cr′ 191.6 (−8.7; −18.6) Cr
1 ($n = 6$)	Cr 140.4 (14.6; 35.4) Cr′ 195.1 (21.8; 46.7) SmA 230.2 (4.1; 8.1) i	i 227.7 (−11.6; −23.2) SmA 187.6 (−18.6; −40.3) Cr′ 175.6 (−21.5; −47.8) Cr
1 ($n = 7$)	Cr 111.4 (8.2; 21.3) Cr′ 197.6 (38.4; 81.7) SmA 228.3 (6.1; 12.1) i	i 223.9 (−6.0; −12.0) SmA 185.8 (−27.0; −58.7) Cr′ 153.8 (−6.0; −14.0) Cr
1 ($n = 8$)	Cr 130.7 (11.3; 8.0) Cr′ 187.4 (43.5; 98.7) SmA 226.9 (17.2; 34.4) i	i 221.1 (−8.6; −17.4) SmA 170.6 (−30.9; −71.2) Cr′ 121.5 (−6.2; −15.6) Cr
1 ($n = 10$)	Cr 121.5 (5.3; 14.0) Cr′ 175.3 (40.7; 90.9) SmA 225.5 (16.2; 32.5) i	i 221.9 (−10.4; −21.0) SmA 168.2 (−27.8; −63.0) Cr′ 136.3 (−9.0; −22.8) Cr
1 ($n = 12$)	Cr 132.7 (70.9; 174.8) Cr′ 171.6 (49.8; 111.9) SmA 221.9 (22.0; 44.7) i	i 219.5 (−18.7; −38.0) SmA 162.3 (−40.3; −92.4) Cr′ 128.8 (−8.2; −20.3) Cr
1 ($n = 14$)	Cr 121.6 (40.2; 101.9) Cr′ 163.4 (27.4; 62.7) SmA 207.7 (6.9; 14.4) i	i 202.9 (−4.2; −8.9) SmA 148.9 (−7.5; −17.8) Cr′ 122.4 (−5.4; 13.7) Cr
1 ($n = 16$)	Cr 136.6 (3.4; 8.2) Cr′ 162.3 (32.5; 74.6) SmA 204.8 (8.8; 18.5) i	i 200.4 (−5.3; −11.1) SmA 152.1 (−22.0; −51.8) Cr′ 132.1 (8.5; 21.0) Cr

[a] Abbreviations: Cr & Cr′ = crystalline state, SmA = smectic A mesophase, i = isotropic liquid.

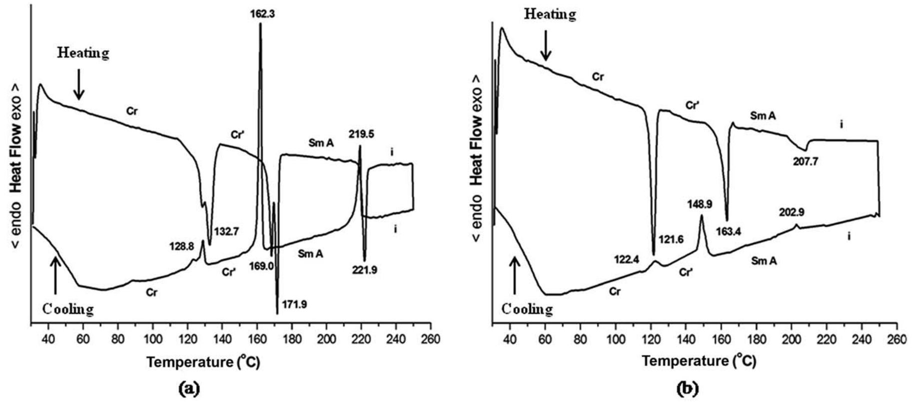

Fig. 2 DSC thermograms of the compound **1** (a) $n = 12$ and (b) $n = 14$ showing enantiotropic mesophase

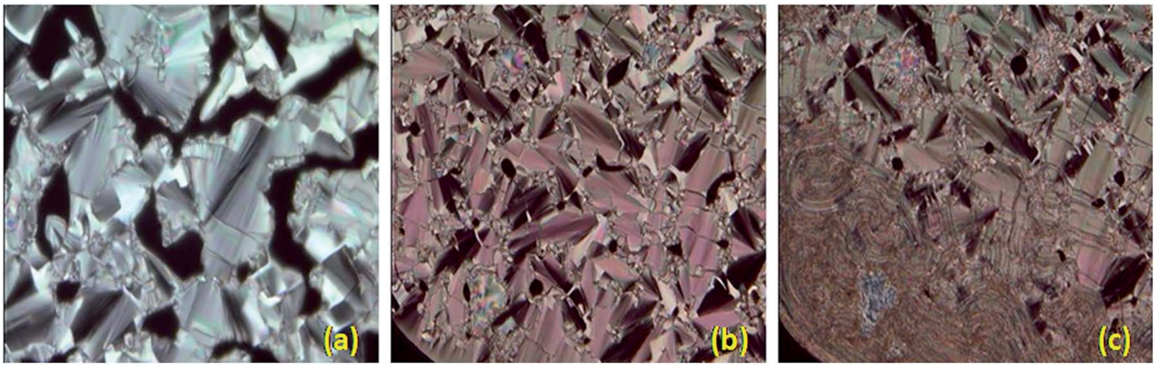

Fig. 3 Microphotographs of the compound **1** ($n = 12$) in SmA phase in cooling cycle (a) broken focal conic texture of compound at 192.1 °C, (b) broken focal conic texture at 184.1 °C and (c) SmA to crystal transition of the compound at 162.2 °C.

XRD measurements were carried out on a representative compound of the series, *viz.*, **1** ($n = 12$) exhibiting a wide range of the mesophase. The raw diffraction profile obtained at a temperature of 200 °C is shown in Fig. 4a. The profile exhibits a sharp intense low angle peak and a weak broad diffuse peak at wide angles, which are characteristic features of a layered

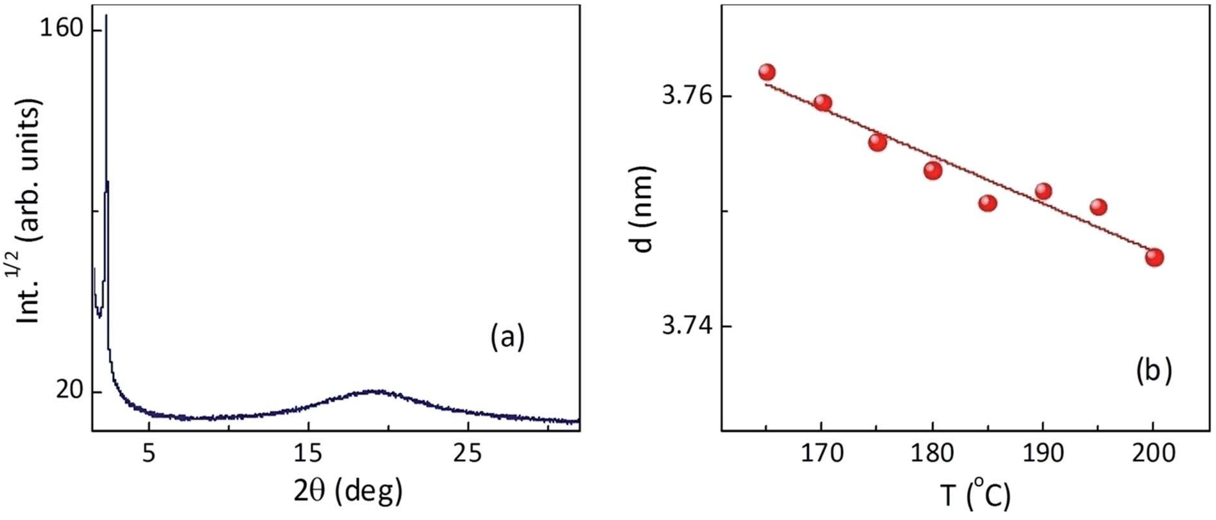

Fig. 4 X-ray measurements on the **1** ($n = 12$) compound. (a) Raw XRD profile collected at 200 °C, exhibiting a sharp low angle peak and a wide angle diffuse maximum. (b) Thermal variation of the layer thickness.

phase. The absence of any higher harmonic peaks corresponding to the low angle peak indicates the layered structure to be of the classical type with a pure sinusoidal density modulation. These features confirm the mesophase to be SmA in agreement with the POM observations. The thermal variation of the layer thickness (d) determined from fitting the low angle peak to a Lorentzian after a proper background treatment, is shown in Fig. 4b. The negative thermal expansion of the layer thickness is not uncommon in the SmA phase. This is caused by the fact that the alkyl chains stretch as the temperature is lowered. The rate of the expansion calculated by the slope d/dT (d) is -4.1×10^{-4} nm K which is typical of monomeric compounds.

The intermolecular hydrogen bond of –C=O···H–N- type has been reported in the compounds containing amide linking group particularly in aryolhydrazones that are responsible for specific supramolecular order of mesogens and also help in mesophase formation.[21,24,27,28] In the view of above fact, temperature dependent Raman spectra of one of the compound **1** (n = 12) have been recorded to verify the presence of intermolecular hydrogen bonding in these systems (Fig. SI 11 and 12†). The temperature dependent variation of C=O stretching and N–H stretching Raman bands is shown in Fig. 5. At room temperature C=O stretching and N–H stretching vibrations at ~1652 and ~3286 cm^{-1} respectively confirm the intermolecular hydrogen bonding between the amide groups.[21,27–29] In Cr–Cr′ transition, both bands shift lower indicating stronger hydrogen bond network. In SmA phase, these bands become broad and shifted higher to 1675 cm^{-1} and 3360 cm^{-1} respectively. This indicates the breaking of hydrogen bonds associated with amide group during crystal to mesophase transition facilitating monomer formation in SmA phase. The calculated length of the optimized structure of monomer (L) is ~49.1 Å (Fig. SI 13†) whereas the interlayer distance d calculated from XRD in SmA phase is ~37.6 Å. In case of $L > d$, the molecular unit in layer is monomeric and intercalation of the alkyl chains of the molecule between the layers exists as shown in Fig. 6.

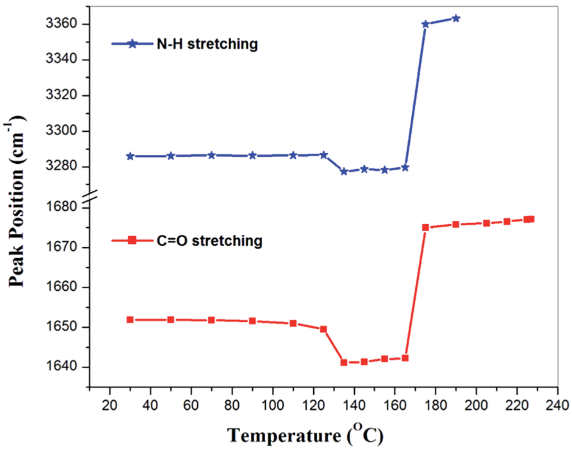

Fig. 5 Peak position variation with temperature of C=O and N–H stretching Raman bands of compound **1** (n = 12).

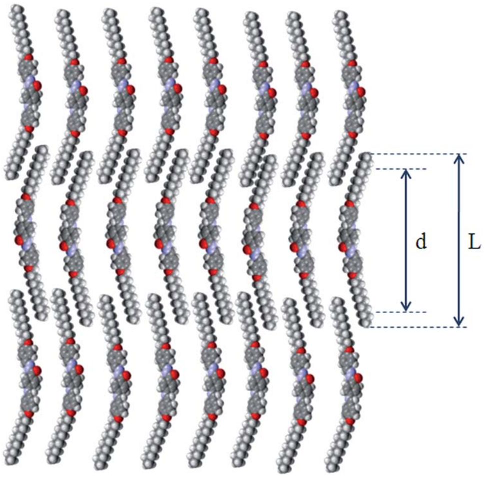

Fig. 6 Schematic representation of molecules in SmA phase.

2.2.2 Compounds with four terminal chains. The compounds **2** (n = 5–8, 10, 12, 14, 16) and **3** (n = 5–8, 10, 12, 14, 16) with four terminal chains at asymmetrical and symmetrical positions (3,4 and 3,5 dialkoxy derivatives) were also prepared to study the effect of side chain density on the formation of mesophases. DSC analysis showed that these compounds with four terminal chains exhibited one single reversible transition in cooling and heating cycles. This single transit in DSC thermograms is assigned to direct melting into isotropic liquid by POM studies. Poor space filling by the four terminal chains for the formation of columnar mesophase is attributed to the non-mesomorphic behaviour of this series of compounds (Table SI 1 and 2†).

XRD patterns obtained for the compounds **2** and **3** (Fig. SI 14†) at temperatures below the isotropic phase displayed several sharp peaks over the whole 2θ ($1° \leq 2\theta \leq 30°$) angular range and confirmed non-mesomorphic character of the material. Interestingly, the lowest angle peak is far more intense than other peaks suggesting that the solid phase may still have a layered ordering with the terminal chains having substantial gauche conformations.

2.2.3 Compounds with six terminal chains. Two classes of compounds with unsymmetrical (2,3,4 trialkoxy) and symmetrical (3,4,5 trialkoxy) carbon chain density (**4** and **5**, n = 5–8, 10, 12, 14, 16) were prepared under this category similar to the compounds with four terminal chains described in the above section in order to verify the role of alkoxy chain density as well as position of terminal chains around the core group for manifestation of mesogenicity in such derivatives. From TGA analysis, the degradation temperature of the compounds **4** and **5** were found to be above 250 °C.

The compounds of the series with unsymmetrical alkoxy chains **4** (n = 5–8, 10, 12, 14, 16) are non mesomorphic and show sharp melting behaviour under POM and DSC studies. XRD patterns obtained for the compounds at temperatures below the isotropic phase displayed several sharp peaks confirmed non-mesomorphic character of the material. The melting point of all the compounds of the series are ranged

Table 2 Thermal transitions and corresponding thermodynamic parameters[a]

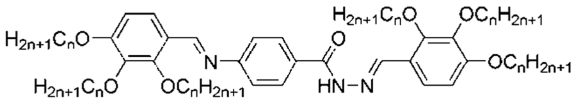

Compound	Heating T, °C [ΔH, kJ mol^{-1}; ΔS, J (mol^{-1} K^{-1})]	Cooling T, °C [ΔH, kJ mol^{-1}; ΔS, J (mol^{-1} K^{-1})]
4 (n = 5)	Cr 78.3 (26.3; 74.7) Cr′ 112.4 (76.3; 197.9) i	i 104.6 (−41.9; −110.9) Cr
4 (n = 6)	Cr 85.9 (15.1; 42.2) Cr′ 103.9 (42.6; 113.0) i	i 99.8 (−36.4; −97.6) Cr
4 (n = 7)	Cr 102.1 (48.3; 128.8) i	i 95.9 (−72.9; −197.5) Cr
4 (n = 8)	Cr 94.7 (79.2; 215.3) i	i 82.9 (−67.7; −190.0) Cr
4 (n = 10)	Cr 82.7 (50.6; 192.9) i	i 72.9 (−60.8; −175.6) Cr
4 (n = 12)	Cr 78.4 (58.4; 166.0) i	i 76.2 (−63.7; −182.4) Cr′ 54.4 (−33.2; −101.3) Cr
4 (n = 14)	Cr 74.3 (64.1; 184.6) i	i 68.5 (−30.3; −88.7) Cr
4 (n = 16)	Cr 58.4 (57.2; 172.5) Cr′ 72.2 (71.4; 206.7) i	i 70.43 (−39.7; −115.6) Cr′ 48.6 (−22.1; −68.8) Cr

[a] Abbreviations: Cr & Cr′ = crystalline state, SmA = smectic A mesophase, $\mathrm{Col_r}$ = rectangular columnar mesophase, i = isotropic liquid.

Table 3 Thermal transitions and corresponding thermodynamic parameters[a]

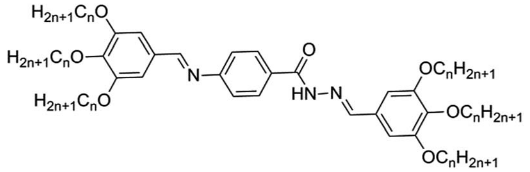

Compound	Heating T, °C [ΔH, kJ mol^{-1}; ΔS, J (mol^{-1} K^{-1})]	Cooling T, °C [ΔH, kJ mol^{-1}; ΔS, J (mol^{-1} K^{-1})]
5 (n = 5)	Cr 124.2 (18.2; 45.7) i	i 120.0 (−14.0; −35.6) Cr
5 (n = 6)	Cr 123.7 (24.5; 61.8) i	i 119.9 (−26.2; −66.6) Cr
5 (n = 7)	Cr 120.2 (21.7; 55.1) i	i 117.4 (−9.8; −25.1) Cr
5 (n = 8)	Cr 113.9 (31.1; 80.3) $\mathrm{Col_r}$ 118.2 (4.0; 10.1) i	i 116.4 (−4.0; −10.3) $\mathrm{Col_r}$ 108.7 (−27.6; −72.2) Cr
5 (n = 10)	Cr 107.9 (28.9; 75.8) $\mathrm{Col_r}$ 114.0 (2.0; 5.3) i	i 111.4 (−2.1; −5.4) $\mathrm{Col_r}$ 100.0 (−25.6; −68.6) Cr
5 (n = 12)	Cr 105.9 (35.5; 93.7) $\mathrm{Col_r}$ 113.3 (8.4; 21.7) i	i 111.0 (−8.3; −21.5) $\mathrm{Col_r}$ 98.8 (−30.5; −82.0) Cr
5 (n = 14)	Cr 96.1 (34.7; 94.0) $\mathrm{Col_r}$ 110.7 (7.2; 18.7) i	i 106.3 (−7.0; −18.4) $\mathrm{Col_r}$ 91.6 (−36.2; −99.2) Cr
5 (n = 16)	Cr 99.0 (40.3; 108.3) $\mathrm{Col_r}$ 109.2 (7.3; 19.2) i	i 105.8 (−6.6; −17.3) $\mathrm{Col_r}$ 92.6 (−32.1; −87.8) Cr

[a] Abbreviations: Cr = crystalline state, $\mathrm{Col_r}$ = rectangular columnar mesophase, i = isotropic liquid.

between 112.4–72.2 °C and 104.6–70.4 °C in heating and cooling cycles respectively as shown in Table 2.

The compounds of the series with symmetrical alkoxy chains **5**(n = 5–8, 10, 12, 14, 16), all exhibited the liquid crystalline behavior of columnar discotics except for short alkyl chain lengths (n = 5, 6 and 7) and were characterized by DSC analysis, POM and XRD studies (for n = 10). The phase transition temperatures and enthalpies of compounds **5** are given in Table 3.

The compounds with octyloxy to hexadecyloxy (n = 8–16) carbon chain length exhibited enantiotropic columnar mesophase. On heating the crystals transform substantially to columnar mesophase above 99.0–113.9 °C, whereas the transition of mesophases at *ca.* 116.3–105.8 °C took place on cooling from the isotropic phase for these compounds (Fig. 7). The columnar rectangular phases of all compounds were easily identified by polarizing optical microscopy (Fig. 8). The compound with decyloxy carbon chain length (n = 10) was also

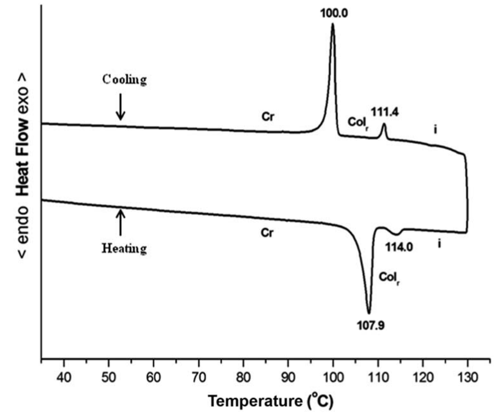

Fig. 7 DSC thermogram of the compound **5** (n = 10) showing enantiotropic mesophase.

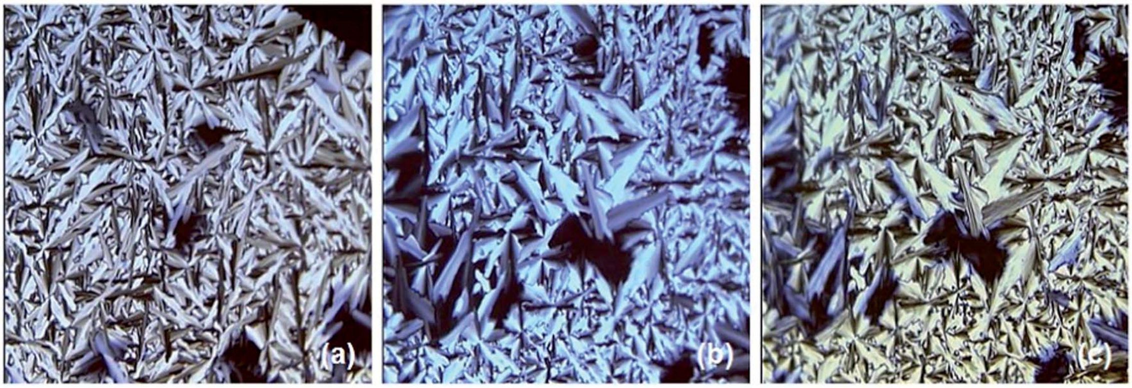

Fig. 8 Microphotographs of the compound **5** ($n = 10$) Col$_r$ phase in cooling cycle (a) at 109.1 °C (b) at 104.2 °C (c) 90.2 °C.

studied by XRD to examine the mesophase structure. Fig. 9 presents the diffraction profile obtained at $T = 100$ °C exhibiting multiple sharp peaks at low angles and a broad diffuse peak at wide angles, clearly points to a columnar phase. The low angle peaks were then indexed; the four reflection indices confirm very well to a rectangular lattice with the (hk) values being (10), (01), (11) and (20); $a = 3.08$ and $b = 2.19$ nm as lattice parameters. The diffuse and broad-scattering halo at wide angle around $d = 0.44$ nm is due to mainly liquid like stacking of the cores along the column with aliphatic chains in a molten state. This columnar rectangular (Col$_r$) mesophase has $p2mm$ plane group symmetry as calculated Miller indices of the observed peaks are such that, $h + k$ is odd as well as even.[30] Such symmetry of rectangular lattice for polycatenar molecules has been observed rarely,[31] only few examples to our knowledge been reported.[28,32–34] The number of molecules forming a columnar unit was found to be as one molecule per columnar unit taking density of the organic molecule as 1 g cm^{-3} and core–core stacking distance as 4.4 Å. According to $p2mm$ symmetry requirements, one molecule is placed at the corner of the columnar unit and these units are stacked to columns, which are organized in a columnar rectangular mesophase. The optimized diameters of disc shape molecule estimated to be around 44.3 Å and 29.4 Å (Fig. SI 15†), indicate that the columns are partial intercalation in the 2D rectangular plane. The N–H stretching Raman band of **5** ($n = 10$) appears at 3340 cm^{-1}, that indicates absence of hydrogen bonding between amides along the column in crystal as well as in columnar phase (Fig. SI 16†). The schematic representation of rectangular arrangement of compound 5 ($n = 10$) in columnar phase is shown in Fig. 10.

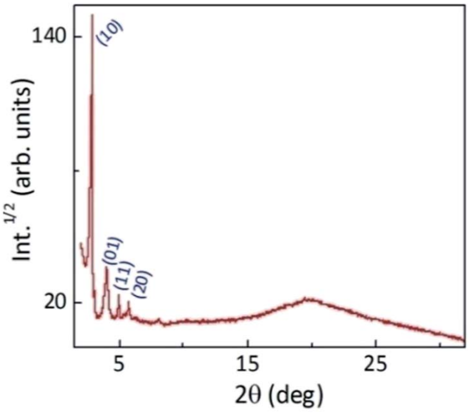

Fig. 9 XRD pattern of the compound **5** ($n = 10$) at 100 °C.

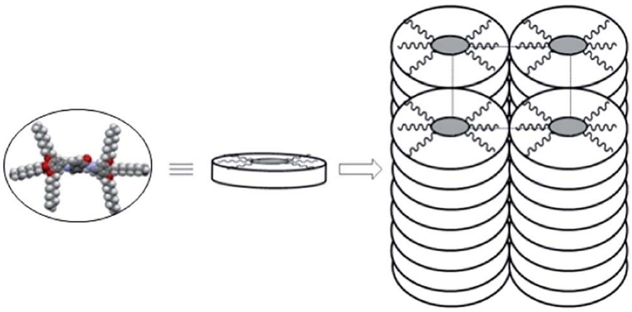

Fig. 10 Schematic representation of columns in which molecules of compound **5** ($n = 10$) self-assemble in a rectangular arrangement.

The homologous series of the compounds **4** with unsymmetrical arrangements *i.e.* 2,3,4 trialkoxy derivatives have lower melting (isotropic) temperature to that it's symmetrical derivatives, **5**. The non mesogenicity of such derivatives may be due to inability of molecule to stack in columns due to asymmetric arrangement of alkoxy terminals. Also, absence of intermolecular hydrogen bonding between layers rules out hexagonal chiral arrangement of molecules as found in earlier similar report on polycatenar derivatives of aroylhydrazone.[21]

Conclusions

We have synthesized lamellar and columnar liquid crystals by substituting peripheral alkoxy benzylidene units at aroylhydrazone core. The mesomorphic behaviors of these compounds were analyzed using various suitable techniques. The compounds with one side chain ($n = 5$–16) at both periphery were found to be mesomorphic in nature, showing SmA mesophase. Temperature dependent XRD, Raman and DFT calculation revealed that these molecules were monomeric in nature with intercalation of alkoxy chains in the SmA mesophase. The compounds with a total of six side chains ($n = 8$–16) at symmetrical position exhibited columnar rectangular mesophase with *p*2*mm* plane group symmetry. However, the compounds with intermediate four side chains are not mesogenic in nature.

The multidisciplinary aspect of this work will be pursued further by complexation of the vacant coordination sites with transition metals in order to endow the resulting material with possible observations of interesting electronic, optical and mesogenic properties due to the presence of metal centre.[35] Work is currently in progress along these lines.

Acknowledgements

HKS (Senior Research Fellow) is grateful to the Council of Scientific and Industrial Research (CSIR), New Delhi, India, for financial support. BS is grateful to DRDO, India (Project no. ERIP/ER/1203053/M/01/1542) and DST, India (Project no. SR/S1/IC-08/2012) for providing financial assistance. RKS is grateful to the DST, India for giving DST-FIST programme under which Raman set-up was procured.

Notes and references

1 D. Matoga, J. Szklarzewicz, K. Stadnicka and M. S. Shongwe, *Inorg. Chem.*, 2007, **46**(22), 9042.
2 K. Hruskova, P. Kovarikova, P. Bendova, P. Haskova, E. Mackova, J. Stariat, A. Vavrova, K. Vavrova and T. Simunek, *Chem. Res. Toxicol.*, 2011, **24**, 290.
3 N. M. H. Salem, L. El-Sayed, S. Foro, W. Haase and M. F. Iskander, *Polyhedron*, 2007, **26**, 4161.
4 P. V. Bernhardt, J. Mattsson and D. R. Richardson, *Inorg. Chem.*, 2006, **45**(2), 752.
5 S. Adsule, V. Barve, D. Chen, F. Ahmed, Q. P. Dou, S. Padhye and F. H. Sarkar, *J. Med. Chem.*, 2006, **49**, 7242.
6 Z. Xu, P. Xi, F. Chen, X. Liu and Z. Zeng, *Transition Met. Chem.*, 2008, **33**, 267.
7 D. K. Johnson, T. B. Murphy, N. J. Rose, W. H. Goodwin and L. Pickart, *Inorg. Chim. Acta*, 1982, **67**, 159.
8 S. Jayasree and K. K. Aravindkshan, *J. Indian Chem. Soc.*, 1994, **71**, 97.
9 L. M. Blinov and S. P. Palto, *Liq. Cryst.*, 2009, **36**(10–11), 1037.
10 N. A. Clark, D. Coleman and J. E. Maclennan, *Liq. Cryst.*, 2000, **27**(7), 985.
11 X. Peng, X. Tang, W. Qin, W. Dou, Y. Guo, J. Zheng, W. Liu and D. Wang, *Dalton Trans.*, 2011, 5271.
12 X. Su and I. Aprahamian, *Chem. Soc. Rev.*, 2014, **43**, 1963 and references cited therein.
13 C. C. Paraschivescu, M. Matache, C. Dobrota, A. Nicolescu, C. Maxim, C. Deleanu, I. C. Farcasanu and N. D. Hadade, *J. Org. Chem.*, 2013, **78**(6), 2670.
14 C. P. Hadjiantoniou-Maroulis, A. J. Maroulis, A. Terzis and D. Mentzafos, *J. Org. Chem.*, 1992, **57**(8), 2252.
15 K. Tran, P. J. Lombardi and J. L. Leighton, *Org. Lett.*, 2008, **10**(14), 3165.
16 G. Majji, S. K. Rout, S. Guin, A. Gogoi and B. K. Patel, *RSC Adv.*, 2014, **4**, 5357.
17 S. Singh, L. K. Sharma, A. Saraswat, I. R. Siddiqui, H. K. Kehrib and R. K. Pal Singh, *RSC Adv.*, 2013, **3**, 4237.
18 M. N. Abser, M. Bellwood, M. C. Holmes and R. W. McCabe, *J. Chem. Soc., Chem. Commun.*, 1993, **13**, 1062.
19 M. N. Abser, M. Bellwood, C. M. Buckley, M. C. Holmes and R. W. McCabe, *J. Mater. Chem.*, 1994, **4**, 1173.
20 C. K. Lai, C. H. Tsai and Y. S. Pang, *J. Mater. Chem.*, 1998, **8**, 1355.
21 G. Shanker, M. Prehm, C. V. Yelamaggad and C. Tschierske, *J. Mater. Chem.*, 2011, **21**, 5307.
22 S. K. Singh, K. Vikram and B. Singh, *Liq. Cryst.*, 2011, **38**, 1117.
23 S. K. Singh, V. Kumar, R. Nandi, H. K. Singh, R. K. Singh and B. Singh, *Liq. Cryst.*, 2015, **42**(2), 222.
24 S. K. Singh, H. K. Singh, R. Nandi, V. Kumar, N. Tarcea, J. Popp, R. K. Singh and B. Singh, *Polyhedron*, 2014, **74**, 99.
25 S. K. Singh, V. Kumar, H. K. Singh, P. Kanth and B. Singh, *Liq. Cryst.*, DOI: 10.1080/02678292.2015.1031717.
26 Z. Galewski, *Mol. Cryst. Liq. Cryst.*, 1994, **249**, 43.
27 T. Kajitani, S. Kohmoto, M. Yamamoto and K. Kishikawa, *Chem. Mater.*, 2004, **16**, 12.
28 G. Shanker, D. S. S. Rao, S. K. Prasad and C. V. Yelamaggad, *RSC Adv.*, 2012, **2**, 1592.
29 H. Shen, K. U. Jeong, M. J. Graham, S. Leng, J. X. Zheng, H. Huang, M. Guo, F. W. Harris and S. Z. D. Cheng, *Soft Matter*, 2006, **2**, 232.
30 N. F. M. Henry and K. Lonsdale, *International Tables for X-ray Crystallography*, 3rd edn, The kinoch press, Birmingham, 1969, vol. I, p. 57.
31 M. Gharbiaa, A. Gharbia, H. T. Nguyenb and J. Malthete, *Curr. Opin. Colloid Interface Sci.*, 2002, **7**, 312.
32 T. Cardinaels, J. Ramaekers, P. Nockemann, K. Driesen, K. V. Hecke, L. V. Meervelt, G. Wang, S. D. Feyter, E. F. Iglesias, D. Guillon, B. Donnio, K. Binnemans and D. W. Bruce, *Soft Matter*, 2008, **4**, 2172.
33 F. Sander, S. Tussetschläger, S. Sauer, M. Kaller, K. V. Axenov and S. Laschat, *Liq. Cryst.*, 2012, **39**(3), 303.
34 C. V. Yelamaggad, G. Shanker, R. V. R. Rao, D. S. S. Rao, S. K. Prasad and V. V. S. Babu, *Chem.–Eur. J.*, 2008, **14**, 10462.
35 J. L. Serrano, *Metallomesogens; Synthesis, Properties and Applications*, VCH, New York, 1996, p. 419.